Climate Resilience of a Large PWR versus an Integral SMR at a Tropical Marine Site: The Role of Regulatory Discharge-Limit Form

*Rachman Bagus Sujiatmoko and Hak-kyu Lim**
Department of NPP Engineering, KEPCO International Nuclear Graduate School 658-91 Haemaji-ro, Seosaeng-myeon, Ulju-gun, Ulsan 45014
rachman.bagus@kings.ac.kr, hklim@kings.ac.kr

***Keywords :** climate resilience; small modular reactor; APR1400; ACP100; thermal-discharge regulation

1. Introduction

Nuclear power plant availability is sensitive to the cooling-water temperature at the condenser intake: a warmer intake raises condenser pressure, reduces the turbine enthalpy drop, and can force a derating under a thermal-discharge limit before the plant reaches any thermodynamic limit [1], [2], [3]. In temperate, river-cooled fleets, the binding constraint in practice is usually this regulatory limit itself, not plant thermodynamics [4], [5], but that literature excludes seawater-cooled plants [6] and has not examined tropical equatorial sites, where the intake baseline already sits close to any plausible discharge ceiling. Indonesia adds a second gap: it has no thermal-discharge standard specific to nuclear power plants, only general marine water-quality rules [7], freshwater thermal-effluent limits [8], and an overarching environmental-management framework [9]. A climate-resilience assessment for an Indonesian site must therefore construct a defensible discharge limit before it can test compliance against it.

This study addresses both gaps together. It compares the climate resilience of a large pressurised-water reactor (APR1400, 1,400 MWe) and an integral small modular reactor (ACP100, 125 MWe) at a candidate marine-cooled site on the Karimata Strait, West Kalimantan, under CMIP6 seawater-temperature projections for 2025–2060 [13],[14], using a discharge limit built by analogy from Indonesia's existing regulations. The objectives are: (i) to quantify the Energy Availability Factor (EAF) and forced-outage duration (N_FO) of both reactors under this constraint; (ii) to determine which constraint, regulatory (f_reg) or thermodynamic (f_thermo), governs the projected availability; and (iii) to test whether the discharge limt's functional form, beyond its numerical level, changes the projected outcome.

The ACP100's integral, passive-safety design is reported to increase safety margin and reduce reliance on external power during accident scenarios relative to large PWRs [18]. Whether these primary-system attributes translate into climate-resilience gains has not been established, since availability under a thermal-discharge constraint is governed by a secondary-side parameter (ΔT_cool) rather than by primary-loop design (Section 3.4). This study isolates that secondary-side channel and quantifies its effect for two specific designs realizing different ΔT_cool values.

2. Methodology

The intake temperature T_in(t) drives two constraints on reactor power: a thermodynamic limit f_thermo(t), set by the condenser energy balance, and a regulatory limit f_reg(t), set by the discharge-temperature standard. Section 2.1 defines both and combines them into the allowable power fraction f_allow(t); Section 2.2 gives the reactor design parameters and the T_in(t) projection used to compute the Energy Availability Factor (EAF) and forced-outage duration (N_FO) over 2025–2060 (Section 3).

2.1 Thermohydraulic and regulatory model chain

The condenser-side chain follows standard condenser energy-balance and isentropic turbine relations [10]: $T_{sat} = T_{in} + \Delta T_{cool} + TTD$, where ΔT_{cool} is the cooling-water temperature rise across the condenser and TTD is the terminal temperature difference between the condensing steam and the cooling-water outlet. T_{sat} fixes the condenser pressure through the IAPWS-IF97 formulation [11], which fixes the turbine enthalpy drop and hence the thermodynamic power fraction f_thermo(t), calibrated so $f_{thermo}(T_{in} = 28°C) = 1$ for each reactor [12]. The regulatory power fraction is $f_{reg}(t) = (T_{max,reg} - T_{in}(t)) / \Delta T_{cool}$, and the allowable power fraction is $f_{allow} = \min [f_{reg}, f_{thermo}, 1.0]$: the plant may deliver only the more restrictive of the two limits.

This formulation assumes once-through cooling at fixed design flow, so that ΔT_{cool} is held constant and compliance is achieved solely by reducing power; discharge temperature is compared directly against the standard. In practice, operators can raise circulating-water flow to lower ΔT_{cool} and thereby increase f_reg. This adaptation is excluded from the results in Table II, which should be read as a design-flow, no-mitigation bound rather than an achievable operating forecast.

BAPETEN has no nuclear-specific discharge standard, so $T_{max,reg} = 33°C$ is built by analogy between Indonesia's marine ambient-water standard (+2°C over ambient, ≈ 31.5°C) [7] and its freshwater thermal-effluent cap (40°C) [8], anchored to the +5°C operational allowance reported at the Barakah NPP [16]. Two forms of this limit are compared in Section 3.3 and Table III: an absolute cap, where f_reg falls as T_in rises, and an incremental limit that tracks ambient

temperature and stays constant. Both forms give the same f_reg at the 28°C baseline; Section 3.3 shows they diverge under warming.

2.2 Design parameters and climate input

Design parameters for the APR1400 (ΔT_cool = 10°C, TTD = 4°C) come from its Design Control Document [15], cross-validated against Barakah NPP data [16]. The ACP100's design cooling-water temperature rise is not published by CNNC/NPIC or by the IAEA ARIS SMR catalogue [17]; ΔT_cool,ACP100 = 8 °C is instead derived from ARIS-confirmed thermal/electrical capacity ($Q_{rej} = Q_{th} - P_0$ = 260 MWt) combined with an assumed condenser circulating-flow rate. This estimate is corroborated by an independent ACP100 secondary-circuit simulation study [19], which reports a two-loop design circulating-water flow of approximately 8350 kg/s; applying this to the same energy balance yields ΔT_cool ≈ 7.4°C, consistent with the 8°C value adopted here. TTD_ACP100 = 5°C remains an unconfirmed assumption, as neither ARIS nor [19] reports the ACP100 condenser terminal temperature difference. Both parameters are therefore treated as engineering estimates, bounded by the sensitivity ranges ΔT_cool = 6-10°C and TTD = 4-6°C applied throughout Section 4. Both reactors are calibrated to a shared 28°C reference intake temperature so that f_thermo (T_in=28°C)=1 for each (Section 2.1); this calibration does not enter f_reg (Section 3.4). The ACP100's regulatory advantage is therefore attributable entirely to its smaller ΔT_cool, and would reverse only if ΔT_cool,ACP100 is in fact ≥ 10°C.

T_in(t) is obtained by a delta method: the CMIP6 (MPI-ESM1-2-LR, thetao) projected anomaly at 10 m depth (linearly interpolated between native model levels) is added to a round-figure T_base = 28°C approximating the regional NOAA OISST v2.1 baseline, which was not independently recomputed for this study. Transferring only the anomaly, rather than the model's absolute climatological state, limits the consequence of using the nearest wet MPI-ESM1-2-LR cell, 68.9 km offshore of the candidate site (1.54°S, 108.68°E vs 1.2°S, 109.2°E), though it does not eliminate that consequence entirely; this is consistent with recent evidence that delta-based bias correction substantially reduces regional CMIP6 sea-surface-temperature bias in the adjacent Indian Ocean [21]. T_in(t) is drawn from a single model at a single grid cell; the reported 95% CI (±0.008°C/yr) reflects single-realization regression uncertainty only and excludes the inter-model structural spread that [20] reports as substantial for this region.

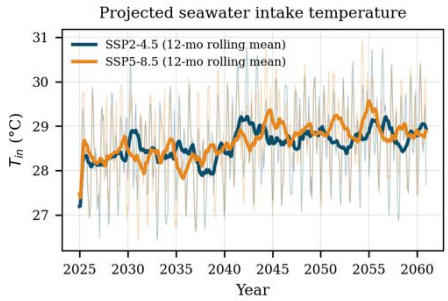


Fig. 1. Projected seawater intake temperature at the candidate grid cell, 2025–2060: raw monthly CMIP6 series (thin) and 12-month rolling mean (thick), both SSP pathways.

3. Results and Discussion

3.1 Baseline design basis

Table I separates each reactor's design basis from the values derived from it at the 28°C reference intake temperature. Both reactors are thermodynamically near-identical: f_thermo stays within 4% of unity across the full projected temperature range, and the ACP100 is in fact marginally more temperature-sensitive on this term alone. The regulatory fraction differs sharply: 0.500 for the APR1400 versus 0.625 for the ACP100, a 12.5-percentage-point gap driven by the smaller ACP100 design ΔT_cool, even though the two reactors have nearly identical thermodynamics — a gap that rests on an assumed rather than confirmed ACP100 design value (Section 2.2).

Table I. Design basis (top) and values derived from it at the 28°C reference intake temperature (bottom).

Parameter	APR1400	ACP100
Design basis		
Rated power	1,400 MWe	125 MWe
ΔT_cool,design	10°C	8°C
TTD	4°C	5°C
Derived at T_in = 28°C		
f_thermo slope	−0.553%/°C	−0.601%/°C
f_reg	0.500	0.625

3.2 Projected EAF and N_FO, 2025–2060

f_reg binds in every one of the 432 projected months for both reactors under both pathways; f_thermo never becomes the limiting constraint (Section 3.3). Table II reports the Energy Availability Factor (EAF, the window-mean f_allow) and the mean forced-outage duration (N_FO, months per year with f_allow below the technical floor f_min,tech = 0.40, an assumed representative value applied identically to both reactors in the absence of a published reactor-specific minimum controlled power level for either unit). The EAF gap holds stable at about 11 percentage points under both pathways, and the APR1400 > ACP100 forced-outage ordering holds across a 0.30–0.50 sensitivity sweep of this floor. Because the ACP100's confirmed technical

minimum has not been published, and the IAEA reports a mechanistic basis for simpler load-following in at least one comparable integral PWR-type SMR design [22], applying an identical 0.4 floor to both reactors is treated here as a conservative-to-the-SMR assumption rather than an established reactor-specific figure; reactor-specific floors, once confirmed, would be expected to widen rather than narrow the reported N_FO gap. This shared-floor treatment is retained pending confirmed minimum-load data for both units.

Table II. Projected EAF and mean forced-outage duration, 2025–2060 window.

Metric	Pathway	APR1400	ACP100
EAF	SSP2-4.5	0.440	0.550
EAF	SSP5-8.5	0.434	0.542
N_FO (mo./yr)	SSP2-4.5	4.0	1.2
N_FO (mo./yr)	SSP5-8.5	4.4	1.3

In physical terms, an 11-percentage-point EAF gap applied to the APR1400's rated capacity corresponds to about 154 MWe of average power output, or roughly 1.35 TWh/yr, a scale planners and regulators can use directly and without price assumptions.

3.3 Why f_reg governs

Fig. 2 plots f_reg(T_in) under both discharge-limit forms and f_thermo(T_in) for both reactors on the same axis. The two families never overlap: f_thermo stays within 0.98–1.01 across the full projected T_in range, while f_reg ranges from 0 to about 0.88 depending on scenario and reactor, always well below f_thermo. This confirms that f_reg, not f_thermo, governs f_allow throughout the 2025–2060 projection, and therefore governs the EAF and N_FO differences in Table II. Let subscript i ∈ {APR1400,ACP100} denote the reactor. Because f_allow = f_reg throughout the window for both reactors, the window-mean EAF reduces algebraically to EAF_i = (T_max,reg - $\bar{T}$_in) / ΔT_cool,i, and the inter-reactor gap to ΔEAF = (T_max,reg − $\bar{T}$_in) · (1 / ΔT_cool,ACP100 − 1 / ΔT_cool,APR1400).

Where $\bar{T}$_in is the window-mean intake temperature. This expression contains no term for reactor power rating, primary-loop layout, or passive safety design: the entire 11-percentage-point gap is carried by ΔT_cool, a secondary-side (condenser/cooling system) design parameter that happens to differ between these two specific units.

The discharge limit, not the turbine cycle, sets how much power this site can deliver.

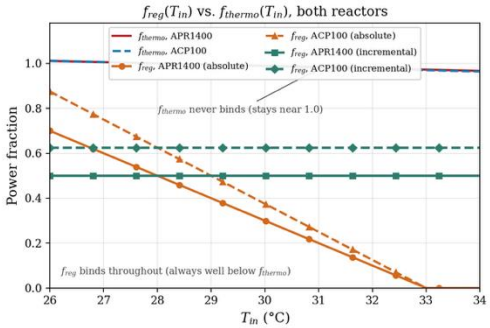


Fig. 2. Regulatory fraction f_reg(T_in) under both discharge-limit forms, and thermodynamic fraction f_thermo(T_in), for both reactors. f_reg stays well below f_thermo across the full projected range, showing why the regulatory constraint always binds first.

3.4 Robustness of the regulatory-form finding

Table III compares f_reg at T_in = 28°C across the stringency range spanned by the two discharge-limit forms. The baseline absolute cap (33°C) and its equivalent incremental form (+5°C) give the same f_reg today, but Fig. 2 shows they diverge under warming, since the incremental form is climate-invariant while the absolute cap erodes linearly. This functional-form effect is larger than the difference between emission pathways, and it is a policy lever more directly within a regulator's control than the emissions trajectory itself. The ACP100 retains the higher allowable fraction under every scenario tested at design flow; this ordering depends on the assumed ΔT_cool,ACP100 value (Section 2.2) and would reverse if ΔT_cool,ACP100 ≥ 10°C.

Table III. f_reg at T_in = 28°C across the tested regulatory-stringency range.

Scenario	Form	f_reg APR1400	f_reg ACP100
Strict, +1.5°C	Incremental	0.15	0.19
Baseline, 33°C / +5°C	Both (equal)	0.50	0.625
Lenient, 35°C	Absolute	0.70	0.875

4. Conclusions

At this site, f_reg binds in every projected month for both reactor classes, while f_thermo stays near-identical between them and never becomes limiting (Section 3.3). The approximately 11-percentage-point EAF gap between the two reactors follows directly from the closed-form decomposition in Section 3.4: it is carried entirely by ΔT_cool, not by reactor power, layout, or safety-system class, and is therefore not itself a climate-sensitive quantity. It remains sensitive to the assumed ΔT_cool,ACP100 value (Section 2.2), which is not yet confirmed by a published CNNC/NPIC design document.

The functional form of the thermal-discharge standard matters as much as its numerical stringency. This finding does not depend on the shared design-

condition assumption: it is a first-order determinant of long-run availability at this site (Section 3.4), within a national regulator's direct control. This extends findings from temperate, river-cooled fleets [4], [5] to a tropical, marine-cooled setting for the first time. As Indonesia develops a nuclear-specific discharge standard, the choice between an absolute and an incremental form deserves treatment as a design decision in its own right.

Two limitations bound these results. First, the assumed $\Delta T_cool,ACP100$ value (Section 2.2); resolving it against a published secondary-side design package is a priority for future work. Second, Table II reports a design-flow, no-mitigation bound (Section 2.1): from the closed form in Section 3.4, an equal flow-adaptation margin would raise f_reg proportionally for both reactors without altering their ordering, but flow adaptation itself is not modeled here and is left for future work.

Acknowledgement

This research was supported by the 2026 Research Fund of KEPCO International Nuclear Graduate School (KINGS), the Republic of Korea.

REFERENCES

[1] K. Linnerud, T. K. Mideksa, and G. S. Eskeland, "The Impact of Climate Change on Nuclear Power Supply," The Energy Journal, vol. 32, no. 1, pp. 149–168, 2011.

[2] A. Durmayaz and O. S. Sogut, "Influence of cooling water temperature on the efficiency of a pressurized-water reactor nuclear-power plant," Int. J. Energy Res., vol. 30, no. 10, pp. 799–810, 2006.

[3] S. I. Attia, "The influence of condenser cooling water temperature on the thermal efficiency of a nuclear power plant," Annals of Nuclear Energy, vol. 80, pp. 371–378, 2015.

[4] Y. Guénand et al., "Climate change impact on nuclear power outages — Part I: A methodology to estimate hydro-thermic environmental constraints on power generation," Energy, vol. 307, art. 132648, 2024.

[5] L. Collet et al., "Future nuclear power outages in a changing climate — A case study on two contrasted French power plants," Energy, vol. 320, art. 135207, 2025.

[6] M. T. H. van Vliet et al., "Global river discharge and water temperature under climate change," Global Environmental Change, vol. 23, no. 2, pp. 450–464, 2013.

[7] Minister of Environment of the Republic of Indonesia, Minister of Environment Decree No. 51 of 2004 concerning Marine Water Quality Standards, 2004.

[8] Minister of Environment of the Republic of Indonesia, Minister of Environment Regulation No. 08 of 2009 concerning Wastewater Quality Standards for Thermal Power Plant Activities, 2009.

[9] President of the Republic of Indonesia, Government Regulation No. 22 of 2021 concerning the Implementation of Environmental Protection and Management, 2021.

[10] Y. A. Cengel and M. A. Boles, Thermodynamics: An Engineering Approach, 8th ed. New York: McGraw-Hill, 2014.

[11] International Association for the Properties of Water and Steam (IAPWS), "Revised Release on the IAPWS Industrial Formulation 1997 for the Thermodynamic Properties of Water and Steam (IAPWS-IF97)," 2012.

[12] N. E. Todreas and M. S. Kazimi, Nuclear Systems Volume I: Thermal Hydraulic Fundamentals, 3rd ed. Boca Raton, FL: CRC Press, 2021.

[13] B. C. O'Neill et al., "The Scenario Model Intercomparison Project (ScenarioMIP) for CMIP6," Geosci. Model Dev., vol. 9, pp. 3461–3482, 2016.

[14] IPCC, "Climate Change 2021: The Physical Science Basis. Contribution of Working Group I to the Sixth Assessment Report," Cambridge University Press, 2021.

[15] Korea Electric Power Corporation (KEPCO) and Korea Hydro & Nuclear Power Co., Ltd. (KHNP), "APR1400 Design Control Document Tier 2, Chapter 10: Steam and Power Conversion System," Doc. No. APR1400-K-X-FS-14002-NP, Rev. 3, Aug. 2018.

[16] B. K. Kim and Y. H. Jeong, "High cooling water temperature effects on design and operational safety of NPPs in the Gulf region," Nuclear Engineering and Technology, vol. 45, no. 7, pp. 961–968, 2013.

[17] International Atomic Energy Agency, "Small Modular Reactor (SMR) Catalogue 2024," IAEA Advanced Reactors Information System (ARIS), Vienna, 2024.

[18] X. Bin, "CNNC's ACP100 SMR: Technique Features and Progress in China," 13th INPRO Dialogue Forum, IAEA Headquarters, Vienna, Oct. 2016.

[19] B.Wang, J. Yang, X. Li, and Y. Yu, "Simulation of ACP100 deaerator operation and response analysis under accident conditions in the secondary circuit system," *Nuclear Engineering and Design*, vol. 456, art. 115000, 2026.

[20] S. Jin, Z. Wei, D. Wang, and T. Xu, "Simulated and projected SST of Asian marginal seas based on CMIP6 models," *Frontiers in Marine Science*, vol. 10, art. 1178974, 2023.

[21] N. D. Sandaruwan Jayarathna, W. Zhou, M. Collins, O. E. Adeyeri, N. Zekai, L. W. A. Erandani, and X. Wang, "Evaluation and future projection of marine heatwaves in CMIP6 models in the Indian Ocean," *Enviromental Research Communications*, 2025, doi: 10.1088/2515-7620/ae21a0.

[22] International Atomic Energy Agency, "Approaches to and Preparation for the Operation of Small Modular Reactors," IAEA-TECDOC-2110, Vienna, 2025.